2. RESULTS AND CONCLUSIONS

Let us now summarize in some detail the principal results of the analysis in Part II of this Report. Accordingly, Section 2 here is organized as follows: first, we briefly consider the first-order results for the phase, ψ, of the narrow-band output of ARI-stages of a typical narrow-band receiver immersed in the general EM interference environment under analysis here [cf. Section (1.1) above]. Next, we present in Section (2.2) various results for the envelope statistics of Class A interference, with a similar presentation in Section (2.3) for the Class B cases. A number of comparisons with experiment are given in Section (2.4), both to demonstrate the canonical character of our models and to exhibit the excellent agreement between theory and experiment which is obtainable by our present analytical approach. Section (2.5) treats the estimation of the physically-based model parameters; Section (2.6) reviews such other results as moments, limiting forms, the existence of Hall models, conditions for the existence of Class A, B, and C noise types, etc. We conclude with remarks in Section (2.7) on uses, advantages, and limitations of these models and outline a number of next steps for their continuing analytical and experimental development.

2.1 Phase Statistics:

In the general case we may use (2.14), Part II, and the relation $W_1(\psi) = \int_0^\infty W_1(E,\psi)dE$, to obtain the pdf, and the APD ($= \int_\psi^\infty W_1(\psi)d\psi$, $(0\leq\psi<2\pi)$), of the instantaneous phase ψ, which will not generally be uniform [on $(0,2\pi)$]. However, in the truly narrow-band situation of Section (2.2)II, we obtain the well-known uniform pdf [(2.21), Part II), e.g. $W_1(\psi)=1/2\pi$, $(0,2\pi)$] as in the simpler, gaussian examples. [Higher-order statistics of ψ, on the other hand, are nonuniform and analytically much more complex: vide Section 9.1.2 of Middleton [1960] in the gaussian cases.] Because of this first-order simplicity for the statistics of the phase we accordingly concentrate our attention on the (first-order) statistics of the associated envelope, which, as expected, departs radically from a gaussian (i.e. rayleigh) behaviour, as our results following, and experiment as well,

amply demonstrate.

2.2 Envelope Statistics: The APD and pdf for Class A Interference:

Our principal analytical results here are: (i), the c.f.; (ii), the PD, or exceedance probability $P_1(\mathcal{E}>\mathcal{E}_o)$; and (iii), the associated pdf, $w_1(\mathcal{E})$. These are respectively*

$$\underline{\text{(c.f.):}} \quad \hat{F}_1(ia\lambda)_A \triangleq e^{-A_A} \sum_{m=0}^{\infty} \frac{A_A^m}{m!} e^{-\hat{\sigma}_{mA}^2 a^2 \lambda^2/2} \quad , \; a^2 = [2\Omega_{2A}(1+\Gamma_A')]^{-1} \quad \text{cf. Eq. (3.3), Part II} \Big\}, \tag{2.1}$$

with $2\hat{\sigma}_{mA}^2 = (m/A_A+\Gamma_A')/(1+\Gamma_A')$, cf. (Eq. (3.5), Part II; and

$$\underline{\text{(PD):}} \quad P_1(\mathcal{E}>\mathcal{E}_o) \simeq e^{-A_A} \sum_{m=0}^{\infty} \frac{A_A^m}{m!} e^{-\mathcal{E}_o^2/2\hat{\sigma}_{mA}^2} \quad , \quad (0 \leq \mathcal{E}_o < \infty), \tag{2.2}$$

cf. Eqs. (3.7a,b), Part II; and

$$\underline{\text{(pdf):}} \quad w_1(\mathcal{E})_A \simeq e^{-A_A} \sum_{m=0}^{\infty} \frac{A_A^m \mathcal{E} e^{-\mathcal{E}^2/2\hat{\sigma}_{mA}^2}}{m! \; \hat{\sigma}_{mA}^2} \quad , \quad (0 \leq \mathcal{E} < \infty) \; , \tag{2.3}$$

cf. Eq. (4.2), Part II. Various curves of P_1, w_1 are given in Figs. (3.1), (3.2), (4.1), (4.2), Part II, showing typical behaviour for selected values of the (global) parameters (A_A, Γ_A'). Here $\mathcal{E}, \mathcal{E}_o$ are normalized envelopes

$$\mathcal{E} \equiv E \Big/ \sqrt{2\Omega_{2A}(1+\Gamma_A')} \quad ; \quad \mathcal{E}_o \equiv E_o \Big/ \sqrt{2\Omega_{2A}(1+\Gamma_A')}, \tag{2.4}$$

cf. Eq. (3.1), Part II, where E_o is some preselected threshold value of the envelope E. (Note that our normalization introduces a third parameter Ω_{2A}.)

The parameters $(A_A, \Gamma_A', \Omega_{2A})$ which appear directly in our statistical results for P_1, w_1 we call "global" parameters. The physical significance of these global parameters $(A_A, \Gamma_A, \Omega_{2A})$ is briefly stated:

---

* See the glossary of principal symbols, at the end of the Report.

1). A_A = the Impulsive Index (for Class A interference): this is defined as the average number of emission "events" impinging on the receiver in question times the mean duration of a typical interfering source emission [cf. Eqs. (2.38), (2.39), Part II and associated discussion]. The smaller A_A, the fewer such events and/or their duration, so that the noise properties are then dominated by the waveform characteristics of a typical event. Loosely speaking, we say that such noise is "impulsive", although here the mean duration of events is sufficiently long to avoid generating noticeable transients in the receiver, i.e. we have Class A noise, as defined above, Section (1.1). As A_A is made large, one approaches gaussian (or in the case of the envelope here), rayleigh statistics (cf. Sec. (2.4), Part II).

2). $\Gamma_A' \equiv \sigma_G^2/\Omega_{2A}$ = the ratio of the intensity of the independent gaussian component σ_G^2 of the input interference including received "front-end" noise, to the intensity Ω_{2A} of the "impulsive", non-gaussian (or rayleigh) component, cf. (3.1a), Part II. A portion, σ_E^2, of this normal component [cf. Sec. (2.3.1), Part II] arises from the cumulative effect of a large number of external sources, none of which is so strong as to be considered part of the "impulsive" interference, which is statistically the dominating effect (for small and moderate Indexes, A_A).

3). Ω_{2A} = the intensity of the above-mentioned "impulsive" component, cf. Eq. (3.1a), Part II.

[The rayleigh nature of P_1, w_1 for large Indexes, i.e., when $A_A \to \infty$, is seen at once from (2.2), (2.3), as then $\Gamma_A' \to \infty$ also, so that $2\hat{\sigma}_{mA}^2 \to 1$, and

$$\therefore \quad P_1(\mathcal{E}>\mathcal{E}_o)_A \to e^{-\mathcal{E}_o^2} \quad ; \quad w_1(\mathcal{E})_A \to 2\mathcal{E}e^{-\mathcal{E}^2} \quad ,(0\leq\mathcal{E}_o,\mathcal{E}\leq\infty), \tag{2.5}$$

in normalized form; see Section (2.4), Part II, for the general case.]

Characteristic behaviour of the APD P_{1-A} vs. $\mathcal{E}_o$, cf. Figs. (3.1), (3.2) [and w_{1-A} vs. $\mathcal{E}$], is exhibited by the "rayleigh" form [constant slope $\eta = -2$, on the linear by $-(1/2)\log_{10}(-\log_e[\ ])$ plots of P_{1-A}] for the comparatively small values of threshold $\mathcal{E}_o$, i.e., large values of $P_1(\mathcal{E} > \mathcal{E}_o)_A$, followed by a very steep rise, after which P_{1-A} bends over and approaches some asymptote with fixed slope η, $0 < \eta < 2$, at large $\mathcal{E}_o$ (small P_{1-A}) less than that of the rayleigh behaviour for P_{1-A} in the 0.1-1.0 region. Thus, we have $P_{1-A} \to e^{-a\mathcal{E}_o^{\eta}}$, $\mathcal{E}_o \to \infty$, $(0<\eta<2)$.

This limiting, finite, and bounded slope as $\mathcal{E}_o$ becomes very large, after the characteristic bend-over, reflects the physical condition that the interference process has finite total <u>average</u> energy; accordingly, no individual source, or finite collection of sources, can emit unbounded energy over any finite period. Furthermore, if the number of sources is <u>finite</u>, with finite <u>power</u>, e.g. no infinite instantaneous amplitudes (as is the case ultimately in practice), then the limiting slope η <u>becomes in-</u>finite at some extremely large value of $\mathcal{E}_o$. This effect can show up at comparatively small values of threshold $\mathcal{E}_o$, for example, with a single, finite source, of limited peak emissions, whereas with multiple sources the phenomenon will occur at larger $\mathcal{E}_o$. In any case, these (below-)bounded slopes (>0) insure, also, that all (finite) <u>moments</u> of the envelope exist, as physically required by the condition of finite average emission energy.

In our models, however, we assume that the number of <u>potential</u> emitting noise sources is infinite, although the probability of even a large number radiating at any given instant is very small, according to the fundamental assumption of poissonian "events", e.g., emissions, postulated here. In addition, we permit a distribution of emission levels ($\sim$ amplitude) per source, where infinite magnitudes are possible, similarly with vanishing probabilities of occurrence. Thus, we may expect a nonzero limiting slope for P_{1-A} as $\mathcal{E}_o \to \infty$: infinite amplitudes can occur, but with vanishing probability*. In practice, however, although the Impulsive Index

---

*The poissonian "rare-event" dominates any "rare-event" from the gaussian component.

(A_A) may be small, there is always the possibility of the very large amplitude "rare event", i.e. $\mathcal{E} > \mathcal{E}_o$(>>0db). But the practical upper limit on $\mathcal{E}_o$ for such an occurrence is so high, i.e., $P_{1\text{-}A}$<0(10^{-8}) or less, usually, that deviation of the experimental results from those predicted by the theoretical models at these levels has not been practically observed. * For example, see Figs. (2.3)-(2.5) following.

2.3 Envelope Statistics: The APD and pdf for Class B Interference:

The Class B interference requires a more extensive analytical model. This arises because two canonical characteristic functions (c.f.'s) are needed to approximate the exact c.f. [vide Section 2.7, Part II], one for small and intermediate values of the envelope ($0 \leq \mathcal{E} \leq \mathcal{E}_B$), the other for the larger values ($\mathcal{E}_B \leq \mathcal{E}$). The principal analytic results here,are, accordingly:

(c.f.'s):
$$\hat{F}_1(ia\lambda)_{B\text{-}I} \doteq e^{-b_{1\alpha}A_B a^{\alpha}\lambda^{\alpha} - \Delta\sigma_G^2 a^2\lambda^2/2}, \quad (0 \leq \mathcal{E} \leq \mathcal{E}_B), \tag{2.6a}$$

$$\hat{F}_1(ia\lambda)_{B\text{-}II} \doteq e^{-A_B \exp[A_B e^{-b_{2\alpha}a^2\lambda^2/2} - \sigma_G^2 a^2\lambda^2/2]}, \quad (\mathcal{E}_B < \mathcal{E} < \infty), \tag{2.6b}$$

from Eqs. (3.10a,b), Part II, with $a^2 = [2\Omega_{2B}(1+\Gamma'_B)]^{-1}$ now, cf. Eq. (3.3), Part II, and

(PD):
$$P_1(\mathcal{E}>\mathcal{E}_o)_B \cong P_1(\mathcal{E}>\mathcal{E}_o)_{B\text{-}I}, \quad (0 \leq \mathcal{E}_o \leq \mathcal{E}_B)$$
$$\simeq P_1(\mathcal{E}>\mathcal{E}_o)_{B\text{-}II}, \quad (\mathcal{E}_B \leq \mathcal{E}_o < \infty) \tag{2.7}$$

Here explicitly we have

---

* We remark, moreover, that our models can be analytically modified to account for a limited, maximum number of emissions at any given instant by truncating the basic summation leading to the usual form [(2.1), Part II] of the characteristic function, cf. Section 2 of Middleton [1974] for details. The functional complexity of the result is, as expected, greatly increased, unless this maximum number is very small.

$$\begin{cases} \hat{P}_1(\hat{\mathcal{E}}>\hat{\mathcal{E}}_o)_{B\text{-}I} \equiv \\ P_1(\mathcal{E}>\mathcal{E}_o)_{B\text{-}I} \simeq 1-\hat{\mathcal{E}}_o^2 \sum_{n=0}^{\infty} \dfrac{(-1)^n \hat{A}_\alpha^n}{n!}\,\Gamma(1+\dfrac{\alpha n}{2})\,{}_1F_1(1+\dfrac{\alpha n}{2};2;-\hat{\mathcal{E}}_o^2)\ , & (2.7a) \\ \\ P_1(\mathcal{E}>\mathcal{E}_o)_{B\text{-}II} \simeq \dfrac{e^{-A_B}}{4G_B^2} \sum_{m=0}^{\infty} \dfrac{A_B^m}{m!}\, e^{-\mathcal{E}_o^2/2\hat{\sigma}_{mB}^2}\ , & (2.7b) \end{cases}$$

with $\hat{A} = A_\alpha/2^\alpha G_B^\alpha$, $\hat{\mathcal{E}}_o \equiv (\mathcal{E}_o N_I)/2G_B$, where

$$\begin{cases} 0 < \alpha < 2; \text{ cf. Eq. (2.82), Part II, et seq.;} & (2.7c) \\ 2\hat{\sigma}_{mB}^2 \equiv (m/\hat{A}_B+\Gamma'_B)/(1+\Gamma'_B),\ \hat{A}_B=(\dfrac{2-\alpha}{4-\alpha})A_B, \text{ cf. Eq. (3.16a), Part II;} & (2.7d) \\ G_B^2 \equiv 2^{-2}(1+\Gamma'_B)^{-1}(\dfrac{4-\alpha}{2-\alpha}+\Gamma'_B), \text{ cf. Eq. (3.12b), Part II .} & (2.7e) \end{cases}$$

The associated pdf's are (from Eqs. (4.3), (4.4), Part II):

$$\begin{cases} w_1(\mathcal{E})_{B\text{-}I} \\ \equiv \hat{w}_1(\hat{\mathcal{E}})_{B\text{-}I} \end{cases} \simeq 2\hat{\mathcal{E}} \sum_{n=o}^{\infty} \dfrac{(-1)^n}{n!}\,\hat{A}_\alpha^n\,\Gamma(1+\dfrac{n\alpha}{2})\,{}_1F_1(1+n\alpha/2;1;-\hat{\mathcal{E}}^2),\ 0 \le \mathcal{E} \le \mathcal{E}_B, \quad (2.8a)$$

$$w_1(\mathcal{E})_{B\text{-}II} \simeq \dfrac{e^{-A_B}}{4G_B^2} \sum_{m=0}^{\infty} \dfrac{A_B^m}{m!}\,\dfrac{\mathcal{E}e^{-\mathcal{E}^2/2\hat{\sigma}_{mB}^2}}{\hat{\sigma}_{mB}^2}\ ,\ (\mathcal{E}_B \le \mathcal{E} < \infty), \quad (2.8b)$$

with ${}_1F_1$, as usual, a confluent hypergeometric function [Middleton, 1960, Appendix A.1.2], so that the $w_1(\mathcal{E})_B = w_1(\mathcal{E})_{B\text{-}I}$ for $0 \le \mathcal{E} \le \mathcal{E}_B$, while $w_1(\mathcal{E}_B) = w_1(\mathcal{E})_{B\text{-}II}$ when $\mathcal{E} \ge \mathcal{E}_B$. In Part II, Figures (3.6), (3.7) show typical curves of the PD, (2.7), and Figures (4.3), (4.4) for the pdf [(2.8a,b)], for selected parameter values. Again, $\mathcal{E}$, $\mathcal{E}_o$ are normalized according to (3.2), Part II, e.g. like (2.4) above, with Ω_{2A} replaced by Ω_{2B}, etc.

There are now <u>six</u> global parameters for our model: $(A_\alpha, \alpha, A_B, \Gamma'_B, \Omega_{2B}; N_I)$, cf. Section 6B (Part II). The subset $(A_B, \Gamma'_B, \Omega_{2B})$ are, just for Class A interference above, respectively, 1), the Impulsive Index; 2), the ratio of the intensity of the independent gaussian component (σ_G^2) to the intensity of the impulsive component; and 3), the intensity of the impulsive component (Ω_{2B}), itself. These have the physical significance described above in Section 2.2. The additional parameters required here are:

4). $A_\alpha = \frac{2\Gamma(1-\alpha/2)}{\Gamma(1+\alpha/2)} \frac{\langle \hat{B}^\alpha_{oB} \rangle}{\{2\Omega_{2B}(1+\Gamma'_B)\}^{\alpha/2}} A_B$ = an "effective" Impulsive Index proportional to the Impulsive Index A_B, cf. (2.38), (2.39), Part II, which depends on the generic parameter α. Here $\langle \hat{B}^\alpha_{oB} \rangle$ is the α-moment of the basic envelope of the output of the composite ARI stages, cf. Fig. (1.1) above, and Eq. (2.87d) Part II.

5). $\alpha \equiv \frac{2-\mu}{\gamma}\Big|_{\text{surface}} ; \frac{3-\mu}{\gamma}\Big|_{\text{vol}}$ = spatial density-propagation parameter, cf. (2.82), Part II et seq.. Here μ, γ are respectively the power law exponents associated with the range dependence of the density distribution of the possibly emitting sources, and their propagation. (See Eq. (2.61) et seq; Section 2.5.2, Eq. (2.63, Part II). The parameter α provides an "effective" measure of the average source density with range. Thus, if we standardize, for example, the propagation law as $\gamma = 1$ (the usual spherical spreading), we have $\mu = 2-\alpha$, $(0<\alpha<2)$, for the source density distribution $\sigma_S \sim \lambda^{-\mu} = \lambda^{\alpha-2}$, ($c\lambda = R$ = distance from a typical source to the receiver). Knowledge of α accordingly gives us a direct measure of effective source density, and if γ is known or measured, separately, then $\mu = 2-\alpha\gamma$ gives us

the actual power law for σ_S, cf. (2.63), Part II. [We shall exploit this relationship in detail in a later study in this series.]

6). N_I = The scaling factor which insure that P_{1-I}, w_{1-I} yields the correct mean square envelope $2\Omega_{2B}(1+\Gamma'_B)$(See Sec. (3.2A).

7). $\mathcal{E}_B = \dfrac{E_B}{\sqrt{2\Omega_{2B}(1+\Gamma'_B)}}$ = the (normalized) "bend-over" point, at which the two (approximate) forms of PD (and pdf) are joined, according to the procedures discussed in Section 3.2, and Eqs. (3.18)-(3.20), cf. Fig. (3.5), Part II. This is an empirically determined point, representing the point of inflexion (for small P_{1-B}) at which the experimentally determined PD, or exceedance probability $P_1(\mathcal{E}>\mathcal{E}_o)_{B\text{-expt.}}$, bends, e.g. at which $d^2P_{1\text{-expt.}}/d\mathcal{E}_B^2 = 0$. Examples of this are indicated in the next Section, (2.4).

We note that without an (experimental) $\mathcal{E}_B$ we cannot predict the limiting form of the PD as $\mathcal{E}_o \to \infty$; we can then only obtain the subset of global parameters $(A_\alpha, \alpha, \Gamma'_B, \Omega_{2B}, N_I))$, cf. Section 6C (Part II). Examples of this are the particular cases of atmospheric and automotive ignition noise shown in Figs. (2.3), (2.4), and interference from a fluourescent light, Fig. (2.5).

The six parameters $(A_\alpha, \alpha, A_B, \Gamma_B, \Omega'_{2B}, N_I)$ are all physically specified and measurable parameters in the analytical model (provided $\mathcal{E}_B$ is determined). Only $\mathcal{E}_B$ itself is an empirical parameter, without explicit quantitative relationship to the underlying physical mechanisms involved. This is because the simplest canonical approximation to the exact c.f. [Eq. (2.87), Part II] requires a two-part c.f., approximate for one to the small and intermediate values of the envelope, and for the other, to the large values

of the envelope. This second c.f., [and PD = $P_1(\mathcal{E} > \mathcal{E}_0)_{B-II}$], provides the needed "bending" of the APD curves for the rare events, as sketched in Fig. (3.5), Part II, for instance, and shown in some of the experimental examples of Section (2.4) following.

Generally, unlike the Class A cases, Class B interference exhibits a much more gradual rise (as $\mathcal{E}_0$ becomes larger), also with increasing α. Similar upward displacement of the rayleigh sections (small $\mathcal{E}_0$) of these APD curves occurs for an increasing gaussian component (Γ_B'), while increasing the Impulsive Index $A_B(\sim A_\alpha)$ also acts to diminish the steepness of these curves as $\mathcal{E}_0$ is increased. The physical necessity for a suitable "bend-over" at the larger values of $\mathcal{E}_0$ has already been discussed above in Section (2.2) for the Class A noise: a fixed, asymptotic slope ($n>0$) is required, to insure the existence of all moments, which in turn is demanded by the condition of finite total average energy. Again, increasing the Impulsive Index and/or increasing the independent gaussian component (σ_G^2) eventually yields a wholly gaussian process (rayleigh, of course, in the envelope), as expected.

2.4 Comparisons with Experiment:

In this subsection we include a variety of comparisons of our theoretical models with experiment, for both Class A and Class B interference, cf. Figs. (2.1)-(2.8) following. Four significant features are at once evident:

(1). The agreement between theory and experiment is excellent, i.e., the approximating forms are effective, analytical relations for predicting the desired first-order statistics;

(2). The canonical nature of our models is demonstrated: the <u>form</u> of the results [here APD's: $P_1(\mathcal{E}>\mathcal{E}_0)$,], is invariant of the specific source mechanism, whether ignition noise, atmospherics, flourescent light, etc., man-made or natural, within the distinct Class A, or B;

(3). Class A and Class B interference are observeably and quantitatively different noise types (vis-à-vis the narrow-band receiver used).

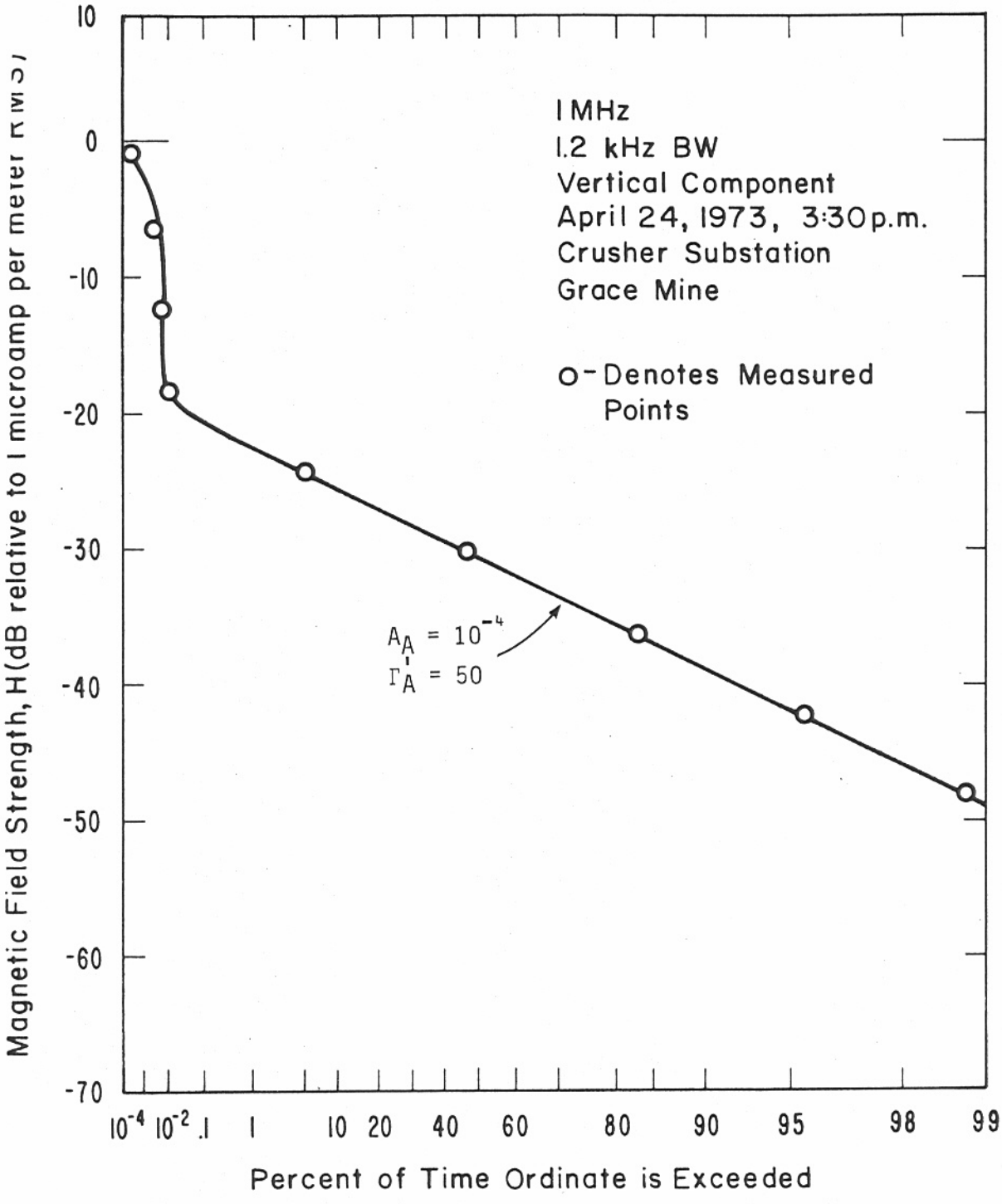

Figure 2.1. Comparison of measured envelope distribution, $P_1(\mathcal{E} > \mathcal{E}_0)_A$, with Class A model, cf. (2.2). Interference from ore-crushing machinery [data from Adams et al (1974)].

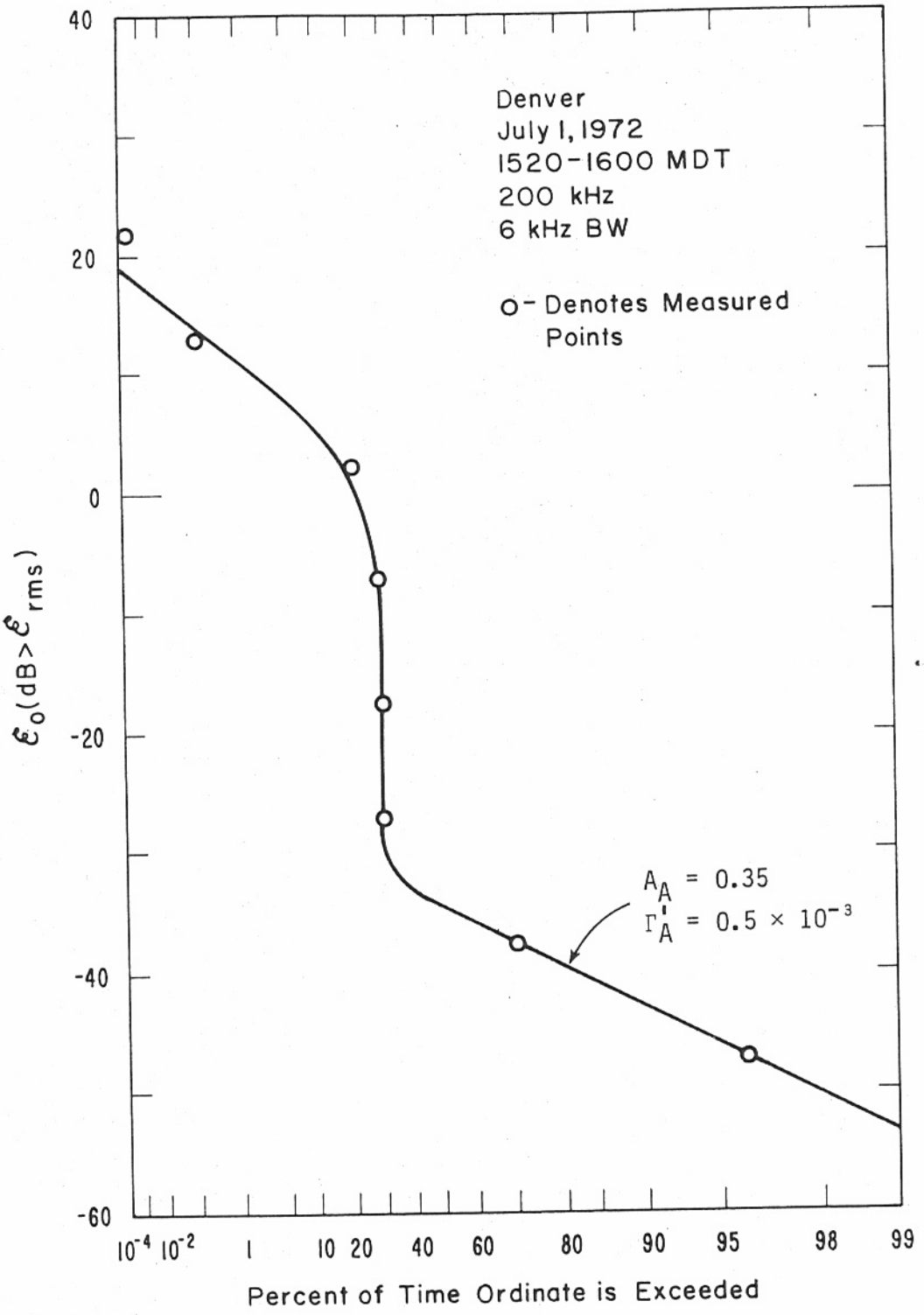

Figure 2.2. Comparison of measured envelope distribution, $P_1(\mathcal{E} > \mathcal{E}_0)_A$, with Class A model, cf. (2.2). Interference (probably) from nearby powerline, produced by some kind of equipment fed by the line [data from Bolton (1972)].

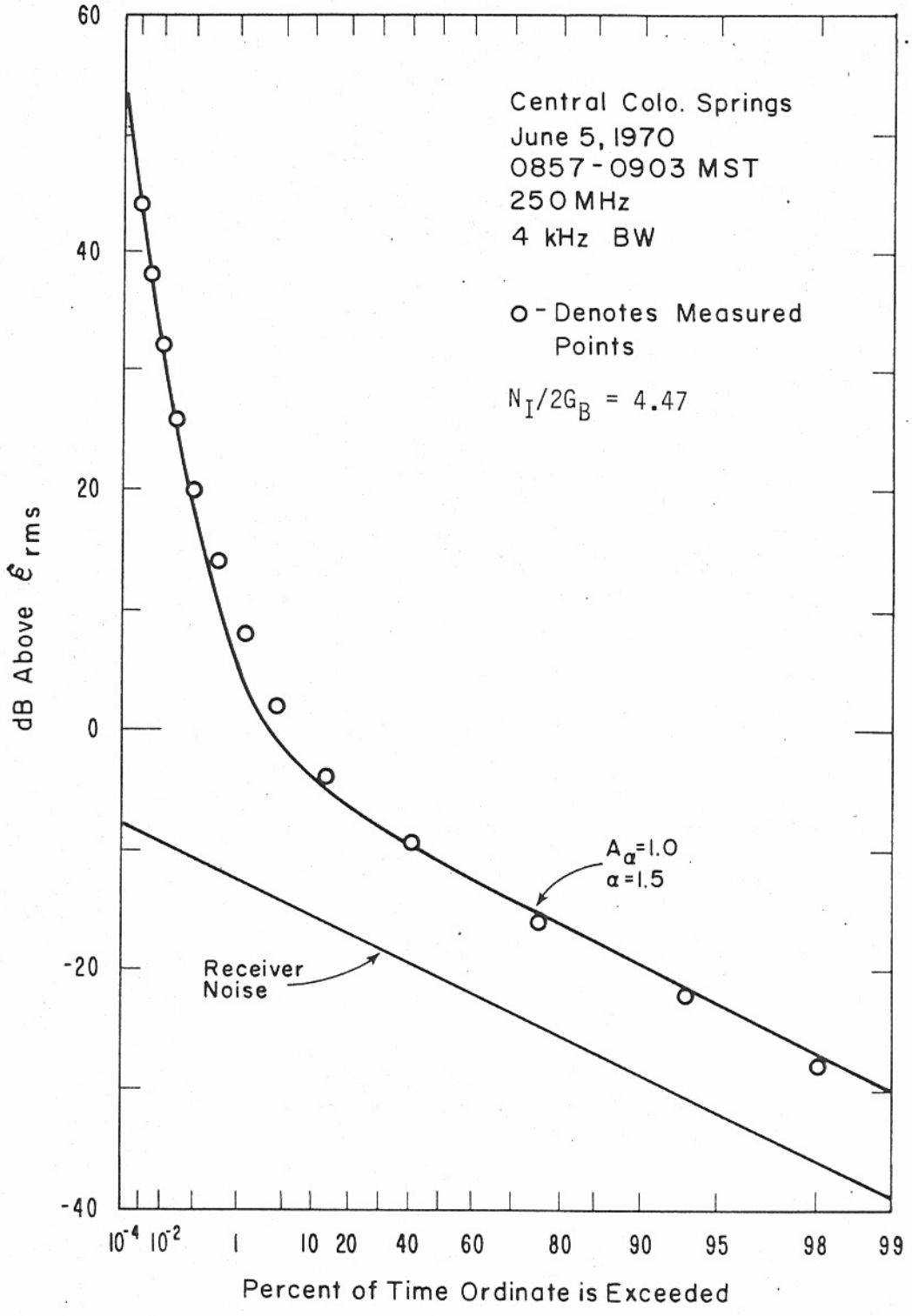

Figure 2.3. Comparison of measured envelope distribution, $P_1(\mathcal{E} > \mathcal{E}_0)_B$, of man-made interference (primarily automotive ignition noise) with Class B model, cf. (2.7a). [Data from Spaulding and Espeland (1971).]

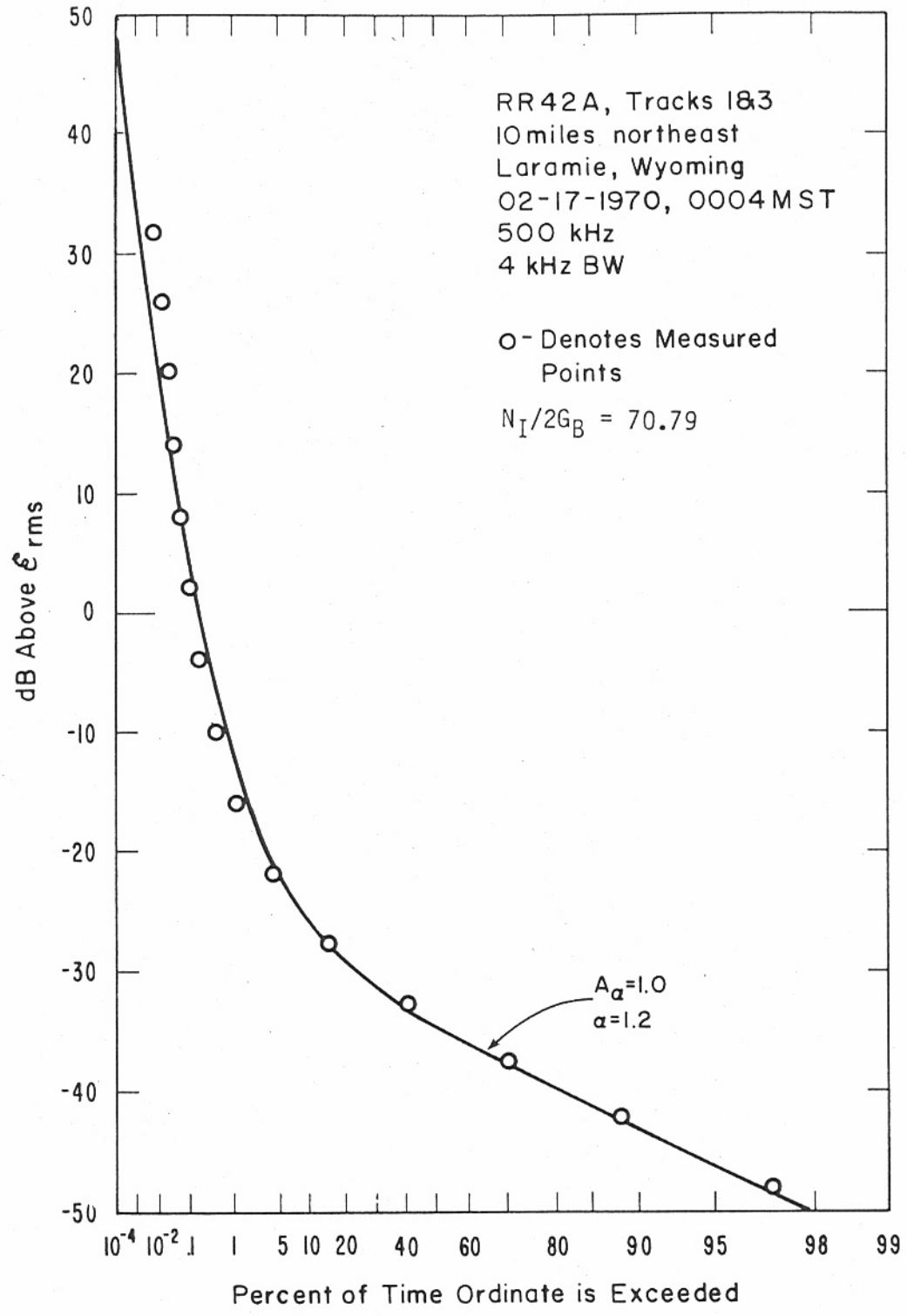

Figure 2.4. Comparison of measured envelope distribution, $P_1(\mathcal{E} > \mathcal{E}_0)_B$, of atmospheric noise with Class B model, cf. (2.7a). [Data from Espeland and Spaulding (1970).]

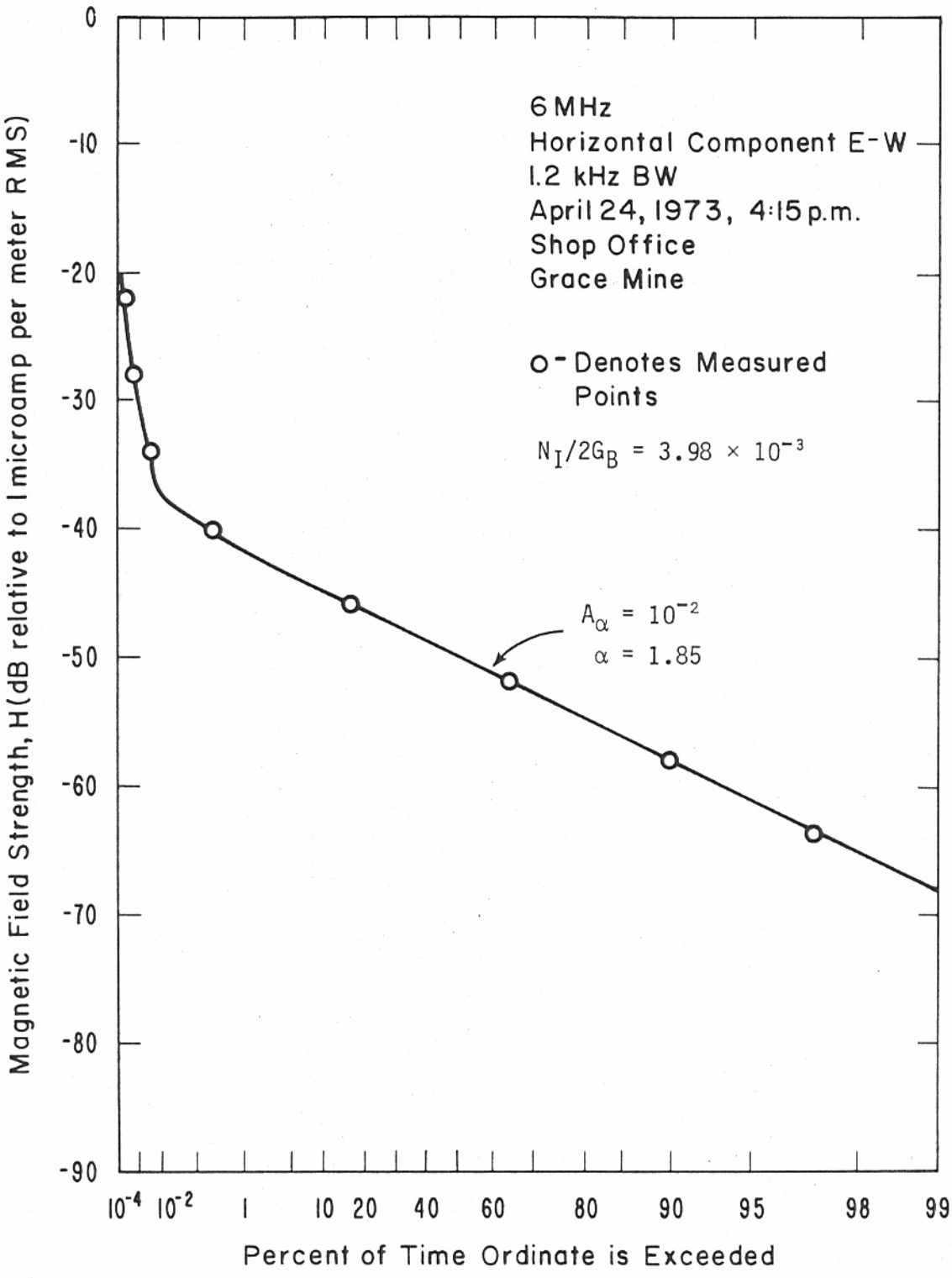

Figure 2.5. Comparison of measured envelope distribution, $P_1(\mathcal{E} > \mathcal{E}_0)_B$ of man-made interference (fluorescent lights in mine shop office) with Class B model, cf. (2.7a). [Data from Adams et al. (1974).]

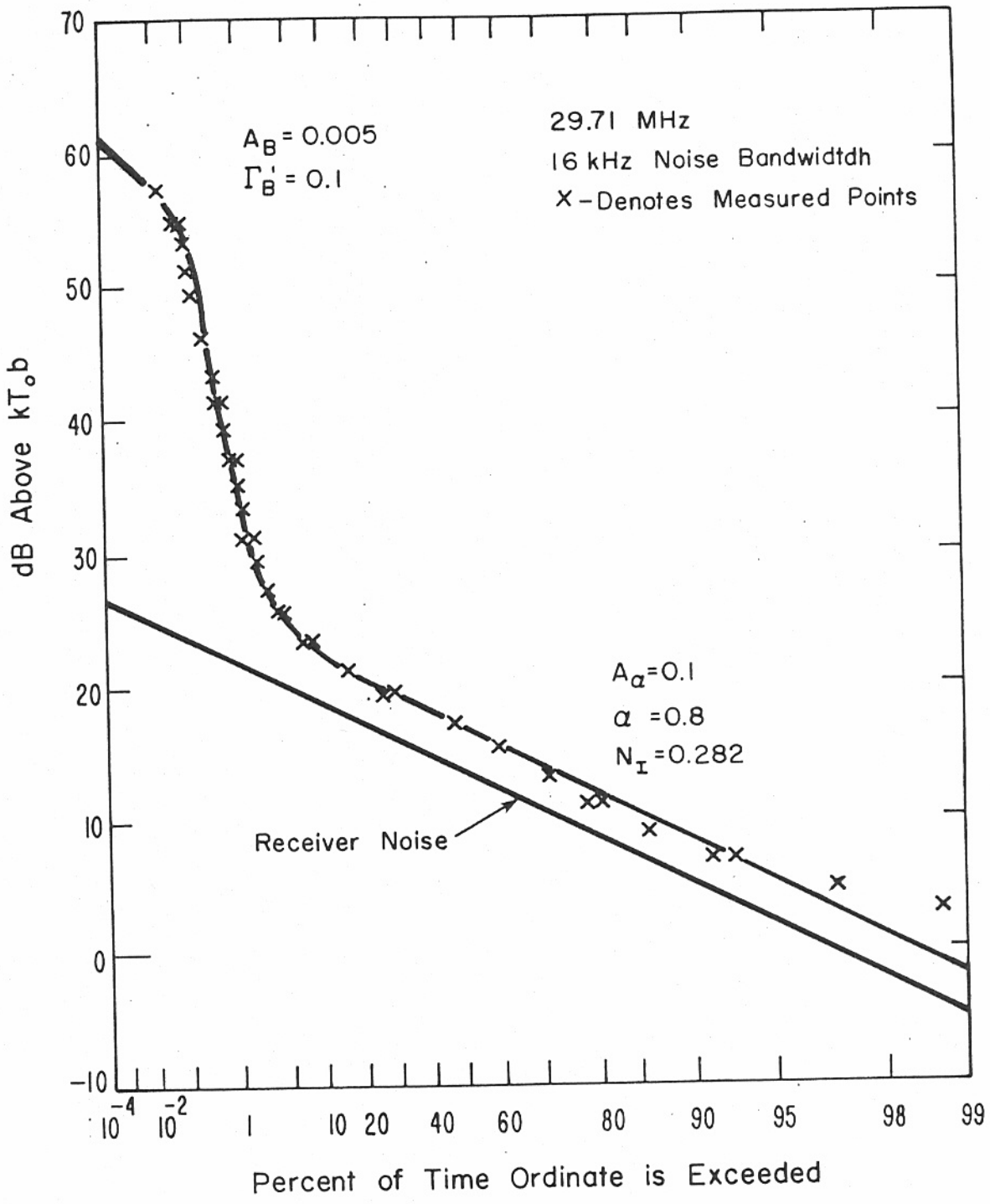

Figure 2.6. Comparison of measured envelope distribution $P_1(\mathcal{E} > \mathcal{E}_0)_B$ of automotive ignition noise from moving traffic with full Class B model, cf. (2.7a,b). [Data from Shepherd (1974), fig. 14.]

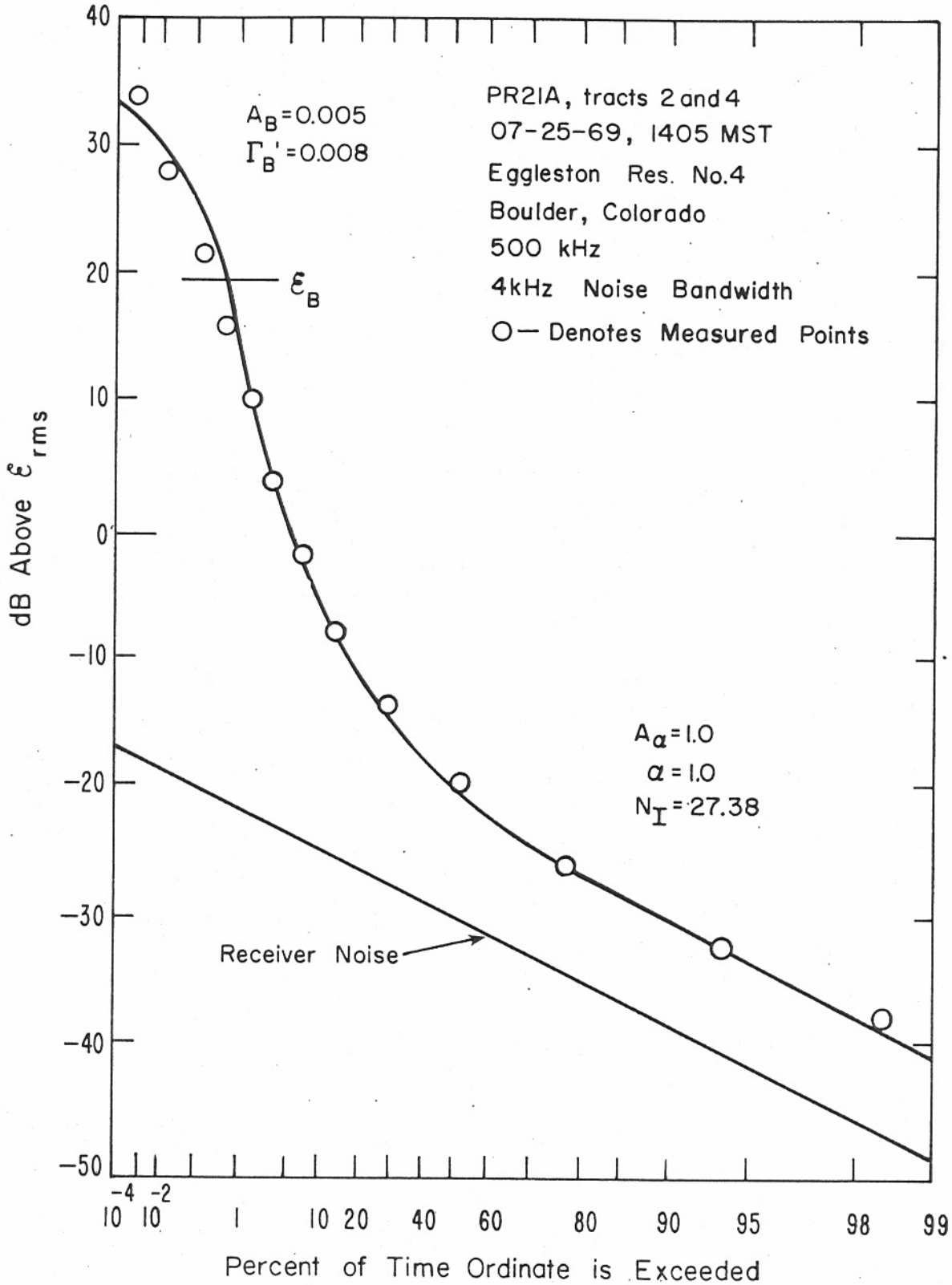

Figure 2.7. Comparison of measured envelope distribution $P_1(\mathcal{E} > \mathcal{E}_0)_B$ of atmospheric noise with full Class B model, cf. (2.7a,b). [Data from Esperland and Spaulding (1970), p. 42.]

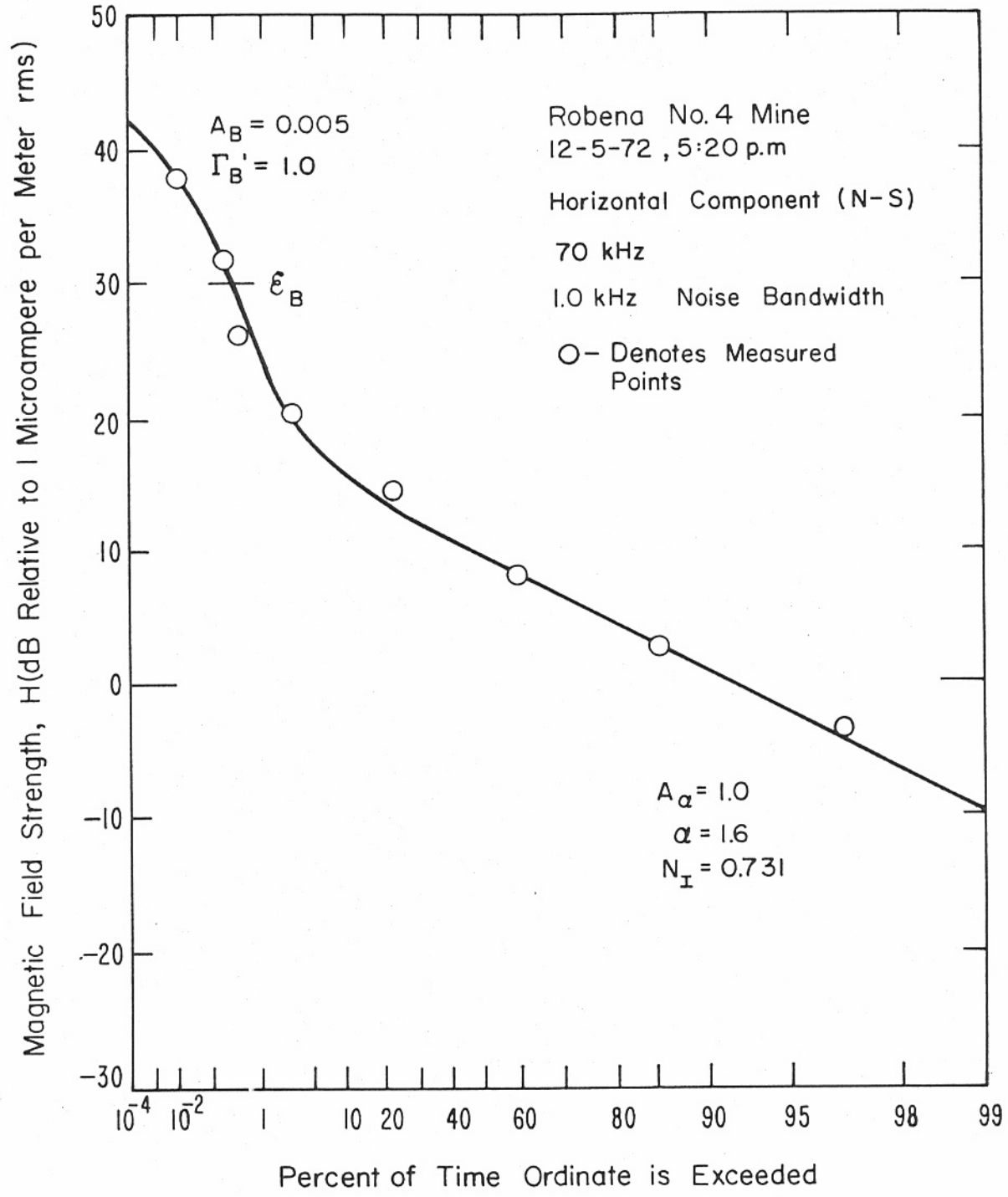

Figure 2.8. Comparison of measured envelope distribution $P_1(\mathcal{E} > \mathcal{E}_0)_B$ of man-made interference (mining machinery noise) with the full Class B model, cf. (2.7a,b). [Data from Bensema et al. (1974), fig. 67, p. 115.]

(4). The governing, physically structured parameters of these PD's and pdf's which are likewise also canonical, can be obtained from approximate experimental data (usually expressed as an APD).

The importance of the canonical character of these models cannot be overstressed: with such models we avoid the very limited and nonpredictive quality of all ad hoc models, whose structure must be verified and whose parameters provide little or no physical insight into the underlying process itself. Second, because these models are derived from physical principles, their parameters are physically defined, are consequently canonical, and are quantifiable in specific instances from empirical data. Their structure, however, is independent of any particular measurement.

Figures (2.1) and (2.2) show APD's, e.g. $P_1(\mathcal{E}>\mathcal{E}_o)_A$ vs. the normalized envelope threshold $\mathcal{E}_o$, for Class A interference, respectively from ore-crushing machining in a mine (data from Adams, Bensema, and Kanda [1974]), and and from a powerline (from E.C. Bolton, [1972]). Observe the characteristic very steep rise following the rayleigh region (constant slope), followed in turn by the expected bending over of the APD for the rarer "events", in each case. [Similar examples of Class A interference, but from man-made, intelligent sources, have also been observed; current experimental studies at ITS, Boulder, are underway to obtain additional such data.]

Figures 2.3-2.5 show APD's of Class B interference, respectively for (i), primarily urban automative ignition noise [Spaulding and Espeland, 1971]; (ii), atmospheric noise [Espeland and Spaulding, 1970]; (iii), flourescent lights, in a mine shop office [Adams et al, 1974]. Observe the more gradual departure from the straight-line rayleigh region, and the continuing rise, with constantly increasing slope in the Figures (which is equivalent to $\eta \to 0$ for $\exp(-a^2\mathcal{E}_o^\eta)$, as $\mathcal{E}_o \to \infty$). [In these particular examples the inevitable "bend over" points $\mathcal{E}_B$, lie outside the range of data taken, e.g. for $P_{1-B}<10^{-6}$, so that we are able to obtain all the global parameters, except for A_B, cf. Sec. 6C, Part II.] This is not the case, however, for the Class B examples of Figs. (2.6)-(2.8), e.g., respectively for (i), ignition noise from vehicles moving on a freeway [Shephard, 1974]; (ii), atmospheric noise [Espeland and Spaulding, 1970];

and (iii), machinery noise in a coal mine [Bensema, Kanda, and Adams, 1974]. Here the required bend-over of the APD's is exhibited, along with the inflexion points, $\mathcal{E}_B$. In these cases we can obtain numerical estimates all the six global (and hence all the generic) parameters characteristic of each example of interference*, man-made or natural, by the methods briefly cited below in Section 2.5, and in more technical detail in Section 6, Part II.

Figures (2.1)-(2.8) are typical of Class A and Class B interference, man-made and natural. They are not intended to be exhaustive. Extensive additional APD data (mostly Class B) are available, for example in Espeland and Spaulding [1970], and Bensema, Kanda and Adams [1974], for example. [We have not included Class C APD data, although these appear in the references cited, because we limit our analysis and comparisons here to the essentially "pure" Class A and Class B interference environment, some (analytical) conditions for which are examined in Sec. 7, Part II.] Again, a striking feature of the present approach is its ability to handle an unlimited variety of noise sources, as long as the dominating Class is identified.

2.5 Remarks on the Estimation of Model Parameters:

We distinguish two sets of model parameters: (a), the so-called global parameters, which appear explicitly in the analytical forms for the APD's, etc. and (b) generic parameters, which are defined directly in terms of the underlying canonical, statistical-physical model. To some extent, both sets overlap. In any case, once the global parameters have been estimated from the data, which usually requires the calculation of the (first-order) APD, the generic parameters can be calculated from them.

The method for obtaining the global parameters is described in detail in Section 6, Part II, and will not be repeated here. However, for convenience, we list the two sets of parameters for each interference Class. These are [from Tables (6.1), (6.2), Part II]:

---

*See footnote added p. 37.

Class A: Global: $(A_A, \Gamma'_A, \Omega_{2A})$; Generic: $(A_A, \sigma_G^2, \langle \hat{B}_{oA}^2 \rangle)$ (2.9)

Class B: Global: $(A_\alpha, \alpha, A_B, \Gamma'_B, \Omega_{2B}; N_I)$; Generic: $(A_B, \alpha, \sigma_G^2, \langle \hat{B}_{oB}^\alpha \rangle, \langle \hat{B}_{oB}^2 \rangle, N_I)$ (2.10)

where, in addition to those parameters described in Sections (2.2), (2.3) above, $\langle \hat{B}_{oA}^2 \rangle, \langle \hat{B}_{oB}^2 \rangle$ are the mean square envelopes of the basic waveforms emitted from the ARI receiver stage, cf. Eqs. (2.64a,b), Part II. Class A noise is described by a three-parameter model, while Class B interference is a six-parameter model globally, and similarly a five-parameter model generically, since the inflexion point ($\mathcal{E}_B$) is empirical and not deriveable here from the fundamental physical model itself. Again, we stress the fact that (except for $\mathcal{E}_B$) all model parameters are physically structured and hence are canonical in form; they are not ad hoc quantities, of strictly limited application.*

Finally, from an examination of the Class B model parameters vis-à-vis those of Class A, we note that (A_A, A_B), (Γ'_A, Γ'_B), and $(\Omega_{2A}, \Omega_{2B})$ are each identical types, of equivalent physical interpretation. The remaining Class B parameters are $(\alpha, \langle \hat{B}_{oB}^\alpha \rangle)$, which provide additional information about the emitting sources, e.g., source density, etc., basic waveshape. Accordingly, it is suggested that to assess the interference environment more fully, in addition to Class A measurements, when possible ARI receiver bandwidths also be selected, to produce Class B interference at the output of the ARI-stage, so as to obtain α and $\langle \hat{B}_{oB}^\alpha \rangle$, in addition to $(A_B, \sigma_G^2, \langle \hat{B}_{oB}^2 \rangle)$, which are analogous to the corresponding Class A set, cf. (2.9). [These $(A_B, \sigma_G^2, \langle \hat{B}_{oB}^2 \rangle)$ are, of course, modified from these Class A counterparts by this choice of ARI bandwidth.] In any case, the important new parameter, α, is obtained, which gives us an estimate of an effective mean source density with range, and the actual one (with range), if the governing propagation law (γ) is also known, or measured, cf. comments following (2.8b) above. Further information about source distributions may be obtained with the help of steerable, directional beam patterns, cf. Section (2.5), Part II. [We shall reserve these questions, in detail, to a succeeding study.]

---

* N_I is not fully dependent on the other generic parameters and is independent of $\mathcal{E}_B$. Hence it may be regarded as generic, cf. Sec. 6B, 6C.

2.6 Some Additional Results:

A brief review of additional results obtained in this Report is now presented. We consider:

(1). First-Order Moments, $\langle \mathcal{E}^{\beta} \rangle$: These are obtained analytically for both Class A and B noise in Section 5 (Part II). They exist for all (real,finite) β, although the (approximate) expressions for the Class B cases are necessarily more complex then for Class A. Alternative, exact, closed-form relations are also obtained for the even integer moments (β=2,4,6,...), cf. Section 5.2 (Part II). [See also the discussion in Section 5.3 (Part II).]

(2). Conditions for Class A,B,C Noise: More precise, analytical conditions are derived in Section 7 (Part II) mutually to distinguish Class A, B, and C interference, than those qualitatively discussed in Section (1.1) above. In general, if the Impulsive Index of one component (A or B) greatly exceeds that of the other (B or A), then the former (A or B) dominates, and we have in practice Class A, or B noise. When this is not the case, the result is the the more general, Class C interference (which we shall treat in a subsequent study).

(3). Approach to Rayleigh Statistics: This occurs when either, or both, the Impulsive Index or the independent gaussian component becomes very large, cf. Section 2.4, Part II. (This is a consequence of the Central Limit Theorem in probability [cf. Section 7.7-3, Middleton, 1960].

(4). Hall Models: A primary empirical model, constructed earlier by Hall [1966], is frequently used for ad hoc representations of the interference environment. Our Class B results, upon deletion of the additive gaussian component (both from the impulsive and independent sources), can be shown to exhibit a Hall form, with Hall parameter (θ_{Hall}=2). [See Section 3.2B, Part II; also, Spaulding and Middleton [1975], Chapter 2.] Such models, however, have a variety of draw-backs, among them being their

ad hoc character, with the parameter(s) entirely empirical, and the non-existence of the second moment, in many instances, as well as the non-existence of all moments $\langle \mathcal{E}^{\beta} \rangle$, where $\beta > \theta_{Hall} - 1$. Their principal advantage is analytic simplicity, which, however, does not ultimately compete with the physical-statistical models of the types developed here. These, though analytically much more involved, are nonetheless still tractable for the purposes of source and system analysis, cf. Spaulding and Middleton [1975]. No Hall models are deriveable from Class A models, however.

(5). Class A vs. Class B Interference: Some Summary Remarks: A concise comparison of some of the salient properties of Class A and Class B interference is presented in Table (2.1):

Table 2.1 Class A vs. Class B Interference

Class A	Class B
1. New Models and Results;	"Classical" (20 Yrs. Old), But New Approach; New Results
2. 3 Global and 3 Generic Parameters $(A_A, \Gamma'_A, \Omega_{2A}) : (A_A, \sigma_G^2, \langle \hat{B}_{oA}^2 \rangle)$	6 Global and Generic Parameters $(A_\alpha, \alpha, A_B, \Gamma'_B, \Omega_{2A}, N_I)$ $(A_B, \alpha, \sigma_G^2, \langle \hat{B}_{oB}^{\alpha} \rangle, \langle \hat{B}_{oB}^2 \rangle, N_I)$ $\mathcal{E}_B$: empirical paramater of approximation
3. All Moments $\langle \mathcal{E}^{\beta} \rangle$, $0 \leq \beta$ exist	All moments $\langle \mathcal{E}^{\beta} \rangle$, $0 \leq \beta$ exist
4. Insensitive to Source Distribution in Space and Propagation Law; Canonical Forms;	Sensitive to Source Distribution and Propagation Law (α); Canonical Forms;
5. Waveform in IF Output: "Gaps" in Time $[P_1(\mathcal{E}=0)>0)$;	Waveform in IF Output: no "Gaps" in Time [e.g. $P(\mathcal{E}=0)=0$];
6. No Gaps in Time if Gaussian Background	No Gaps in Time ($\sigma_G^2 > 0$);
$\left\{ \begin{matrix} X & \text{Gauss P.D.} \\ \mathcal{E} & \text{Rayleigh P.D.} \end{matrix} \right\}$ as $A_A \to \infty$; and/or $\sigma_G^2 \to \infty$	$\left\{ \begin{matrix} X & \text{Gauss P.D.} \\ \mathcal{E} & \text{Rayleigh P.D.} \end{matrix} \right\}$ as $(A_\alpha, A_B) \to \infty$; and/or $\sigma_G^2 \to \infty$
7. No Hall Models Exist;	Hall Models for Special Values of α; (Gauss Component Absent)

2.7 General Comments; Next Steps:

In the preceeding sections we have summarized the principal results of our present study of the (first-order) envelope and phase statistics of man-made and natural electromagnetic interference, whatever its physical origins and characteristics. These analytical models, of Class A and B interference, are mathematically tractible and canonical in application: the forms of the results, and the number, type, and general structure of the associated parameters, are invariant of the particular source. Of course, particular parameter values do depend on the specific properties of the particular source involved. These are estimated in turn, by general procedures outlined here., cf. Section 2.5 above, and Section 6, Part II from experimental data, principally the APD [= exceedance probability $P_1(\mathcal{E}>\mathcal{E}_0)2$. The canonical character of these models and their parameters is derived from the general underlying physical structure upon which the models are based. This, in turn, is itself a general space-time model of propagation, source distribution, and emission [Middleton, 1974, and Section 2, and principally Secs. 2.1,2,5, Part II here].

As expected, the resulting statistics of amplitude and envelope are highly nongaussian (or nonrayleigh), as the analysis and examples in Part II and the experimental results of Section (2.4) indicate. This necessarily has a critical effect on conventional receiver and system operation, which may be in conventional usage, (approximately) optimized, e.g. "matched", to desired signals in gaussian noise (so-called correlation receivers and their extensions), but which is radically suboptimum for this kind of electromagnetic environment [Spaulding and Middleton, 1975].

Here we are concerned with first-order interference statistics themselves, not only for purposes of system design, optimization, and comparison, but also for the tasks of measuring and assessing the properties of EM interference fields. Excellent agreement between model and observation has been found, as the examples of Section 2.4 above demonstrate. In addition, explicit numerical results are also obtained for the global and generic parameters of the interference phenomenon in question, e.g., automotive ignition noise, communications, atmospherics, machinery, power line emissions and the like. These parameter values, along with the basic

physical structure, permit us to deduce general properties of the interference field, such as average source distribution in space (α), emission density in time (Impulsive Index, A), mean intensity (Ω_2), the amount of external gaussian noise (σ_G^2), etc., and, of course, the associated APD, or exceedance probability $P_1(\mathcal{E}>\mathcal{E}_0)$, as well as various moments ($\langle\mathcal{E}^\beta\rangle$) of the interference process.

First-order statistics of these highly nongaussian EM noise environments as embodied in the APD, $P_1(\mathcal{E}> \mathcal{E}_0)$, $P_1(X>X_0)$, for example are, however, minimal for the proper treatment of the general class of communication systems operating in such environments. In many situations the performance bounds established from these first-order statistics are quite adequate [the independent sample cases of Spaulding and Middleton, 1975, for example], where higher-order time structures are not significant. However, when they are, one clearly needs appropriate extensions of the present models. In addition, the joint statistics of signals and noise are also required, of first- and higher-orders as well. Therefore, as part of our continuing effort to develop an applicable analytic description of the EM nongaussian interference environment, we present the following program, in approximate order of undertaking:

I. Interference Models (present series):

1). Report, Part III: First-order statistics of the instantaneous amplitude (X) for Class B noise, e.g., $P_1(X>X_0)_B$, $w_1(X>X_0)_B$, moments, parameter estimates, etc. (now underway).

2). Report, Part IV: First-order statistics of Class C noise, envelope (E) and instantaneous amplitude (X), e.g. $P_1(X>X_0)_C$, $P_1(\mathcal{E}>\mathcal{E}_0)_C$, etc., with experimental comparisons.

3). Report (possibly Part V) on measurements, parameter estimates, and description of EM interference environments. This will include evaluation of selected, earlier data [for example, Furutsu and Ishida, 1960, Espeland and Spaulding, 1970; Shephard, 1974], and comparisons with our models. This may also include recommendations for van usage and area coverage, etc.

4). Report, on simulation of EM environments, to establish robustness and sensitivity of the various models to modifications in their

structure.

5). Report, on various special problems and extensions of Part I-IV, for example, to develop the analysis for Class B noise when $\alpha = 0, \alpha \geq 2$, including other source distributions. Also, we need to examine the case of a single source at known positions [Shephard, 1974]. The rôle of the "corrections" [Middleton, 1974] requires further clarification, etc.

6). Report on mean and variance of "zero-crossings" for Class A,B,C interference. These statistics are useful adjuncts to the APD's to provide some insight into the time-structure of the interference.

7). Report on the first-order statistics (envelope, phase, and instantaneous amplitude) of Class A and B interference with a general, additive signal present at the input to the typical narrowband receiver.

8). Report on the development of higher-order (principally 2nd-order) pdf's for Class A, B, C noise; possibly including signals as well.

II. Performance and Optimum Systems in General EM Interference Environments: (series with Spaulding and Middleton [1975]).

1). Report (Part II): Optimum reception with Class B interference; this is now underway);

2). Report (Part III): extension of the above to Class C cases;

3). Report, on the analysis of other specific systems in Class A and B noise; the improvement of performance bounds, the specification of LOBD receiver structures, and further extensions of the evaluation process.

These lists are not, of course, complete, nor will the program itself necessarily be carried out in the order indicated, since some of these topics may shift in priority as time goes on. In any case, however, the general goal of developing an applicable analytical theory, tested by experiment, for these general classes of man-made and natural, highly

nongaussian, electromagnetic noise or interference processes, may be considered a major priority task for the future in the science and technology of telecommunications.

2.8 Acknowledgements

The author wishes to thank Dr. A. D. Spaulding of the Office of Telecommunications for his constructive discussions and criticisms of this material and for performing the numerical calculations and developing the figures contained in this report.

---

*Note that $\Gamma_B' \equiv \sigma_G^2/\Omega_{2B}$, where σ_G^2 is the independent gaussian component, which is different from the total gauss component $\Delta\sigma_G^2 = \sigma_G^2 + b_{2\alpha}A_B$, cf., eq. (2.88a). Thus, in Figs. 2.6, 2.8 we must calculate Ω_{2B} from the data curve and then obtain σ_G^2 from Γ_B'. From the other parameters in these figures all the remaining generic parameters are then readily found. On the other hand, for Fig. 2.7 Ω_{2B} occurs at 0 dB, by normalization. Since P_1=0.36 determines the total gauss component ($\Delta\sigma_G^2$ for Class B, σ_G^2 for Class A noise), from the data of Fig. 2.7 we get $\Delta\sigma_G^2 \doteq$ -17 dB (=2.10^{-2}) and $\therefore \sigma_G^2 = \Gamma_B'\Omega_{2B} = 10\log_{10}(8.10^{-3}) \doteq$ -21 dB, which gives in turn $b_{2\alpha}A_B \doteq 0.012$ (in units of Ω_{2B}). Again, all remaining generic parameters are now obtainable, from this and the other parameter data on Fig. 2.7 (also in units of Ω_{2B} here).